



UNIVERSITY OF LEEDS

This is a repository copy of *Biomimetic Curvature and Tension-Driven Membrane Fusion Induced by Silica Nanoparticles*.

White Rose Research Online URL for this paper:

<https://eprints.whiterose.ac.uk/181043/>

Version: Supplemental Material

Article:

Arribas Perez, M and Beales, PA orcid.org/0000-0001-9076-9793 (2021) Biomimetic Curvature and Tension-Driven Membrane Fusion Induced by Silica Nanoparticles. *Langmuir*, 37 (47). pp. 13917-13931. ISSN 0743-7463

<https://doi.org/10.1021/acs.langmuir.1c02492>

© 2021 American Chemical Society. This is an author produced version of an article, published in *Langmuir*. Uploaded in accordance with the publisher's self-archiving policy.

Reuse

Items deposited in White Rose Research Online are protected by copyright, with all rights reserved unless indicated otherwise. They may be downloaded and/or printed for private study, or other acts as permitted by national copyright laws. The publisher or other rights holders may allow further reproduction and re-use of the full text version. This is indicated by the licence information on the White Rose Research Online record for the item.

Takedown

If you consider content in White Rose Research Online to be in breach of UK law, please notify us by emailing eprints@whiterose.ac.uk including the URL of the record and the reason for the withdrawal request.



eprints@whiterose.ac.uk
<https://eprints.whiterose.ac.uk/>

Biomimetic curvature and tension-driven membrane fusion induced by silica nanoparticles

Marcos Arribas Perez¹ and Paul A. Beales^{1,2,}*

¹ Astbury Centre for Structural Molecular Biology and School of Chemistry, University of Leeds, Leeds, LS2 9JT, UK.

² Bragg Centre for Materials Research, University of Leeds, Leeds, LS2 9JT, UK.

* Correspondence: p.a.beales@leeds.ac.uk

Keywords: Artificial cells, membrane remodelling, bionanotechnology, lipid bilayers, lipid mixing, membrane biophysics.

Supporting information

SiO₂ NPs characterisation

Figure S1. Size distribution analysis of SiO₂ NPs from transmission electron microscopy (TEM) images.

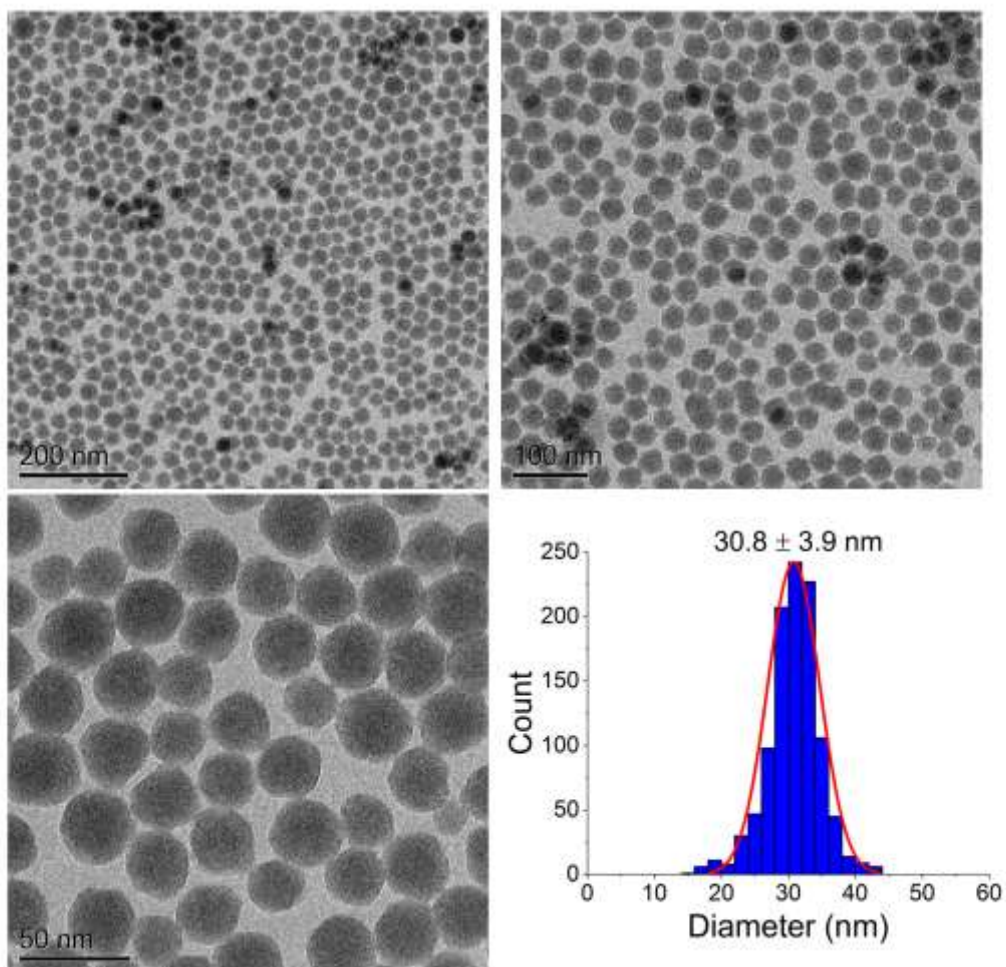
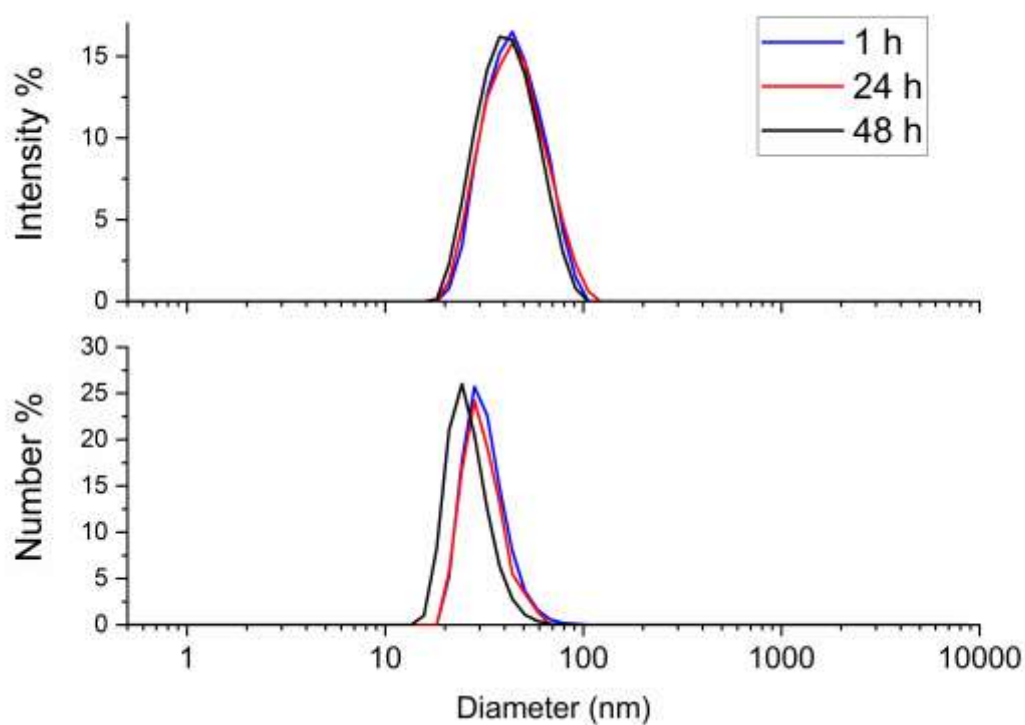


Figure S2: Size distribution (by intensity and by number) and colloidal stability of SiO₂ NPs measured by DLS. Data in the table indicates the mean hydrodynamic diameter of SiO₂ NPs obtained from 3 independent measurements.



Incubation time	Distribution by intensity (diameter in nm)	Distribution by number (diameter in nm)
1 hour	43.0 ± 2.4	28.4 ± 3.2
24 hours	42.6 ± 2.6	27.6 ± 2.2
48 hours	38.8 ± 1.8	24.5 ± 3.6

Fusion of LUVs mediated by SiO₂ NPs

Figure S3. [Left] Example of fluorescence emission spectrum of DOPC LUVs labelled with 0.25 mol% Rh-DOPE and NBD exposed to different concentrations of SiO₂ NPs for 30 min (Max fusion control sample made of LUVs labelled with 0.05 mol% Rh-DOPE and NBD). [Right] Average FRET ratio and FRET efficiency at a range of SiO₂ NP concentrations after 30 min incubation with LUVs.

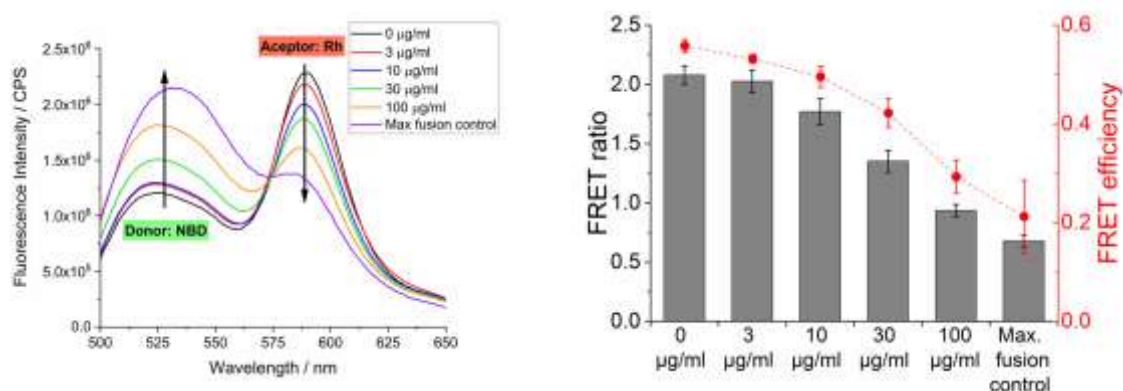
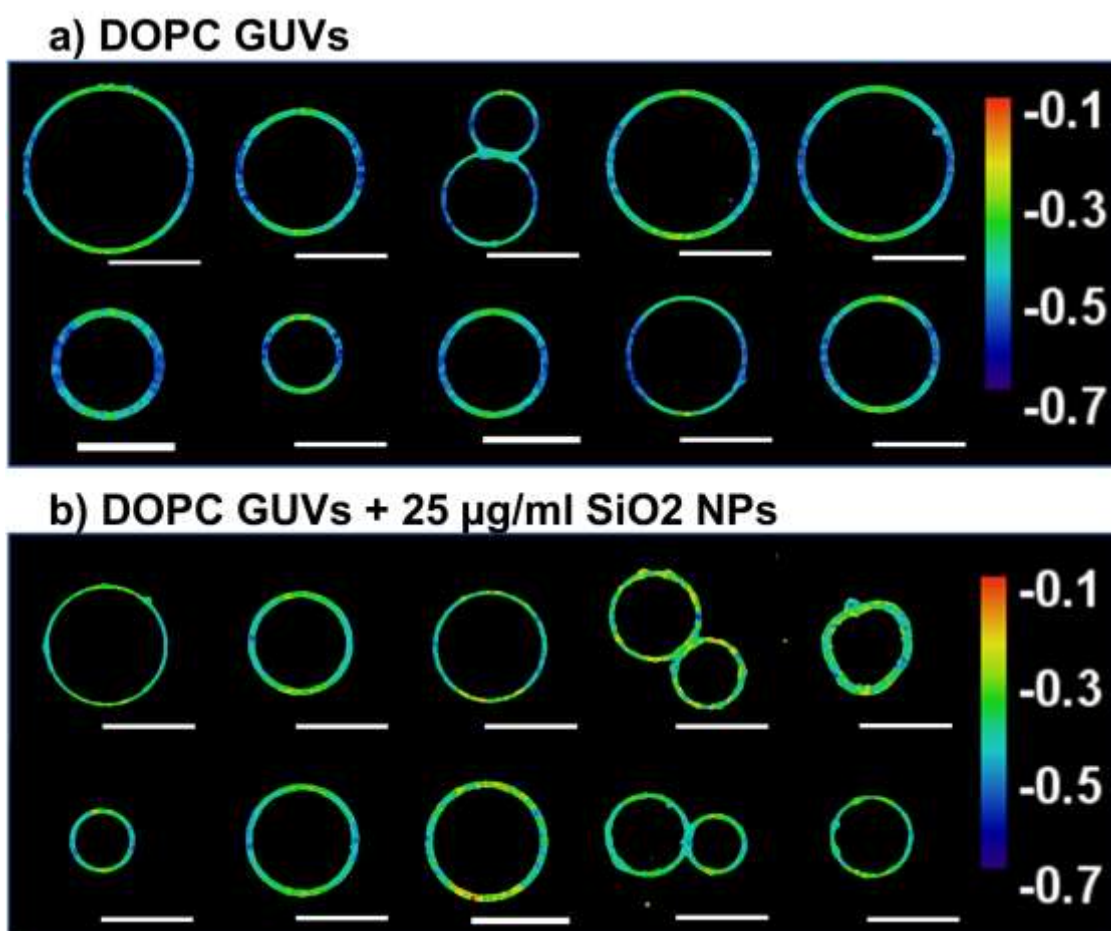


Table S1. Hydrodynamic diameter of DOPC LUVs after exposure to different concentrations of SiO₂ NPs for 30 min. (Cumulants fit, size distribution by intensity)

	Replicate 1	Replicate 2	Replicate 3	Average ± SD
LUVs (0 µg/ml SiO₂ NPs)	333.50 nm	361.60 nm	347.20 nm	347.40 ± 14.05 nm
LUV + 30 µg/ml SiO₂ NPs	451.00 nm	454.70 nm	542.9 nm	482.90 ± 52.02 nm
LUV + 100 µg/ml SiO₂ NPs	589.80 nm	557.90 nm	544.60 nm	564.10 ± 23.23 nm

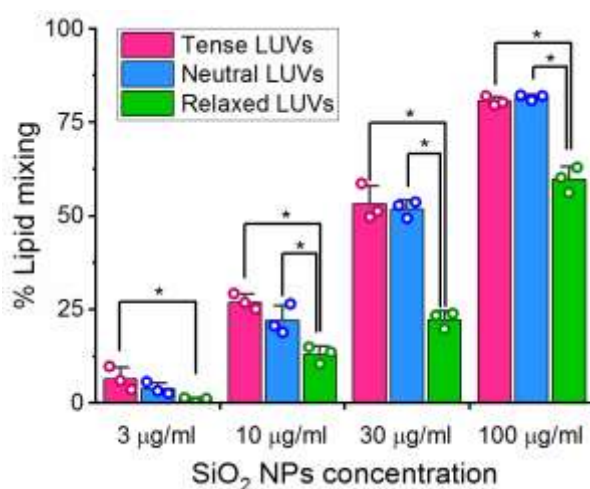
Laurdan GP maps of DOPC GUVs before and after exposure to SiO₂ NPs

Figure S4. Laurdan GP maps obtained from spectral images of DOPC GUVs labelled with 0.5 mol% Laurdan before (a) and after (b) incubation with 25 $\mu\text{g}/\text{ml}$ SiO₂ NPs. 10 different images are shown for each condition. Higher GP values displayed at the top of the GUVs in all the images are attributed to an artifact associated to the light polarisation which produce different fluorescence intensities in the equator and the poles of the GUVs. After incubation with SiO₂ NPs we do not detect localised regions with significant increased GP values but the GP maps show slightly increased GP values across the whole GUV contour.



Influence of membrane tension in the fusion efficiency of LUVs

Figure S5. Effect of membrane tension on the fusion efficiency of LUVs after exposure to SiO₂ NPs for 30 min, measured by FRET. Tense LUVs, Neutral LUVs and Relaxed LUVs were incubated overnight in hypotonic (-10 mOsm/kg), isotonic, and hypertonic (+10 mOsm/kg) buffer (20 mM HEPES, 150 mM NaCl, pH 7.4), respectively before conducting the experiment. The results show a significantly lower percentage of lipid mixing in samples of relaxed LUVs. No significant difference observed between Tense and Neutral LUVs, probably because the neutral LUVs are already very tense after being extruded and the $\pm 3\%$ osmolarity difference used in these experiments is deliberately small so that these differences do not directly induce topological changes in the GUVs by themselves. The bars show the mean, the error bars the standard deviation and circles indicate each individual measurement. The statistical significance was tested using a one-way ANOVA with a post-hoc Bonferroni test (*p < 0.05)

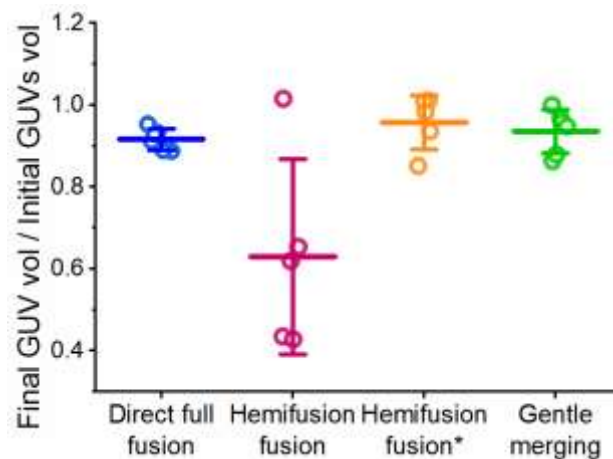


Change of GUVs volume upon fusion

Figure S6. Ratio of volume between the final GUV and the two initial GUVs during the different fusion pathways. From confocal microscopy time series, we measured the diameter of the GUVs at the beginning and the end of the fusion process to calculate their volume. The change of GUV volume is reported as the ratio between the volume of the final fused GUV and the sum of the volume of the two initial GUVs.

$$\frac{\text{Volume of final GUV}}{\text{Volume of initial GUV 1} + \text{Volume of initial GUV 2}}$$

If this ratio is 1, the volume of the two initial GUVs is conserved in the final GUV, while lower values indicate volume loss during the fusion process. During the direct full fusion and gentle merging pathways there is volume conservation (direct full fusion = 0.92 ± 0.03 ; gentle merging = 0.93 ± 0.05). These pathways generate a final GUV with a volume that is approximately equivalent to the sum of the volumes of the initial GUVs. On the other hand, during the hemifusion-fusion pathway there is a significant loss of volume in the final GUV in comparison to the GUVs at the beginning of the fusion process (0.63 ± 0.24). In this case, we also analysed the change in volume between the final GUV and the GUVs at the time just before the fusion pore opens (denoted as Hemifusion-fusion*) and observed that the opening of the fusion pore is not associated with a volume reduction (0.96 ± 0.07), but the loss of volume occurs while the GUVs are hemifused. The data is presented in the plot as mean \pm standard deviation and circles indicate each individual measurement.



Supplementary movies

File Name: Supplementary Movie 1

Description: Sequential fusions of homogeneously labelled GUVs (Rhodamine-DOPE used as fluorescence dye). First fusion *via* gentle merging pathway and second fusion *via* hemifusion-fusion pathway (colour code scale indicated fluorescence intensity)

File Name: Supplementary Movie 2

Description: Fusion of homogeneously labelled GUVs *via* direct full fusion (Rhodamine-DOPE used as fluorescence dye) (colour code scale indicated fluorescence intensity)

File Name: Supplementary Movie 3

Description: Fusion of GUVs lumen mediated by SiO₂ NPs *via* hemifusion-fusion pathway (Magenta and green fluorescence correspond to DiD, DiO and TRITC-dextran, respectively)

File Name: Supplementary Movie 4

Description: Fusion of differently labelled GUVs mediated by SiO₂ NPs *via* direct full fusion pathway (Red and green fluorescence correspond to Rhodamine-DOPE and DiO, respectively)

File Name: Supplementary Movie 5

Description: Fusion of differently labelled GUVs mediated by SiO₂ NPs *via* hemifusion-fusion pathway. (Red and green fluorescence correspond to Rhodamine-DOPE and DiO, respectively)

File Name: Supplementary Movie 6

Description: Fusion of differently labelled GUVs mediated by SiO₂ NPs *via* gentle merging pathway. (Red and green fluorescence correspond to Rhodamine-DOPE and DiO, respectively)